https://doi.org/10.5194/essd-2026-242
Preprint. Discussion started: 20 April 2026

Open Access Earth System Science Data Discussions

TReAD: 40-year Taiwan Reanalysis Downscaling Dataset at 2 km

Chao-Tzuen Cheng [a], Chihchung Chou [a], Ping-Yi Lin [a], Huang-Hsiung Hsu [b], Yung-Ming Chen [a]

[a] National Science and Technology Center for Disaster Reduction, New Taipei City, Taiwan

[b] Research Center for Environmental Changes, Academia Sinica, Taipei, Taiwan

Correspondence to: Chihchung Chou (ccchou84@gmail.com)

Abstract

There has been an increasing demand to reconstruct long-term gridded Essential Climate Variables (ECVs) for climate-change impact and application studies, especially for the regions with highly complex topography like Taiwan. Furthermore, the need for climatic variables like wind speed, relative humidity, etc has been rapidly increasing for diverse application research mainly because sparsely distributed station-based observation data cannot fulfill the requirement. This paper introduces the Taiwan Reanalysis Downscaling data (TReAD) that re-forecasts a range of ECVs with 2-km resolution for Taiwan from 1980 to 2019. Forced with the European ReAnalysis (ERA5), TReAD was generated by dynamically downscaling simulations using the Weather Research and Forecasting (WRF) model. Overall, TReAD shows a comparable long-term trend seen in the ground-based observation data while biases can still be seen mostly in mountainous regions. Moreover, the ranking of the six ECVs in terms of overall performance (taking into account correlation coefficients and deviations) is atmospheric pressure, temperature, relative humidity, shortwave radiation, wind velocity and precipitation. As for reproducing extreme weather events such as typhoons, TReAD reasonably captured the temporal and spatial variability of precipitation observed for Morakot in 2009. To our knowledge, TReAD is the first high-resolution long-term historical climate reconstruction for Taiwan and has been applied in climate-related studies. For instance, TReAD has been found to be a valuable (higher weights) data source particularly in gauge-scarce areas when developing a multi-source precipitation product in the hydroclimatic field. What's more, the impact of typhoons on cloud forests has been assessed by using TReAD's wind velocity that could not be achieved using gauge-based observation data alone. It is important to highlight that TReAD not only can resolve the effect of the complex terrain in Taiwan but also make many more climate variables available for the foreseen climate-related studies. The datasets are freely available for download via the SciDM platform (Cheng et al., 2025, https://doi.org/10.30193/scidm-rs-2576295).

https://doi.org/10.5194/essd-2026-242
Preprint. Discussion started: 20 April 2026

Keywords: historical climate reconstruction, Taiwan, climate change, high resolution, dynamically downscaling

1. Introduction

The availability and length of observational station data sets have been among the important needs for climate change and its subsequent impact studies. Especially, to quantitatively evaluate simulated climatic variables in a relatively small domain like Taiwan with high spatial variability, the data set needs to be of higher resolution and comprehensively cover the entire domain. There are three main challenges of conducting climate change-related research for Taiwan: firstly, sparsely distributed in-situ observation stations are mostly located over land rather than the surrounding oceans; furthermore, the stations in mountainous regions are much lacking than on the plain; lastly, the spatial resolutions of global General Circulation Models (GCMs) or reanalysis data sets are too low to be applied in Taiwan where its complexity of topography is high. These issues are explained in detail as follows.

Since the length of the record of observational stations is often short, even lacking, particularly over the oceanic and mountainous areas (Cheng et al., 2016). Although satellite telemetry can provide spatially dense data with uniform distribution, its short period limits the following evaluation and value-added applications such as climate analysis of long-term trend. To tackle this issue, reanalysis data generated using atmospheric dynamic models are frequently one of the alternative solutions. Global reanalysis data are constructed by assimilating GCMs simulations and observation datasets and they can provide three-dimensional gridded data with a reasonable atmospheric condition/pattern that is not easily captured by models alone. Furthermore, many research institutes have released their own reanalysis data and have continually updated along with the GCM upgrades. For example, the frequently used reanalysis datasets include ERA5 released by the European Centre for Medium-Range Weather Forecasts (ECMWF) (Hersbach et al., 2018a, 2018b, 2020); R-1 (Kalnay et al., 1996), R-2 (Kanamitsu et al., 2002), CFSR (Saha et al., 2010) generated by the U.S. National Centers for Environmental Prediction (NCEP); and JRA-55 generated by the Japan Meteorological Agency (Ebita et al., 2011; Kobayashi et al., 2015).

Although global reanalysis data can fulfill the requirements of long-term time period and comprehensive spatial domain (e.g., the global ERA5 attains a relatively high horizontal resolution of 0.25 degree), it still fails to adequately capture the details of regional atmospheric patterns. Especially, Taiwan has a highly variable topography i.e., the altitude ranges between 0-3000 m in 140 km (east-west width) as shown in Figure 1. Such topography makes regional-scale climate

https://doi.org/10.5194/essd-2026-242
Preprint. Discussion started: 20 April 2026

analysis and application studies more difficult (Chen et al., 2007). Another challenge when working on the regional climate in Taiwan is that the majority of the observation stations are located on the western plain (see Figure 1). This problem might lead to the difficulty of understanding the climatic condition in the mountainous regions.

The objective of this study is to reconstruct high-resolution historical climate data over Taiwan and the surrounding ocean via dynamically downscaling 40-year ERA5. Kanamitsu and Kanamaru (2007) produced a 10-km resolution dataset by dynamically downscaling the 57-year NCEP/NCAR reanalysis 1 using a regional climate model. Moreover, the results showed that the reconstructed data is of high quality and comparable to the regional analysis, NARR (Kanamaru and Kanamitsu, 2007). Similarly, Kayaba et al. (2016) used the 55-year JRA-55 to conduct dynamic downscaling and recreated a 5-km resolution dataset. As such, the dynamic downscaling has been proven to effectively produce historical data of climatic variables like temperature, rainfall, even extreme weather events for the regions with complicated terrain in particular. Therefore, we have followed the aforementioned logics and reconstructed a set of historical climate data over Taiwan at 2-km resolution for the period from 1980 to 2019.

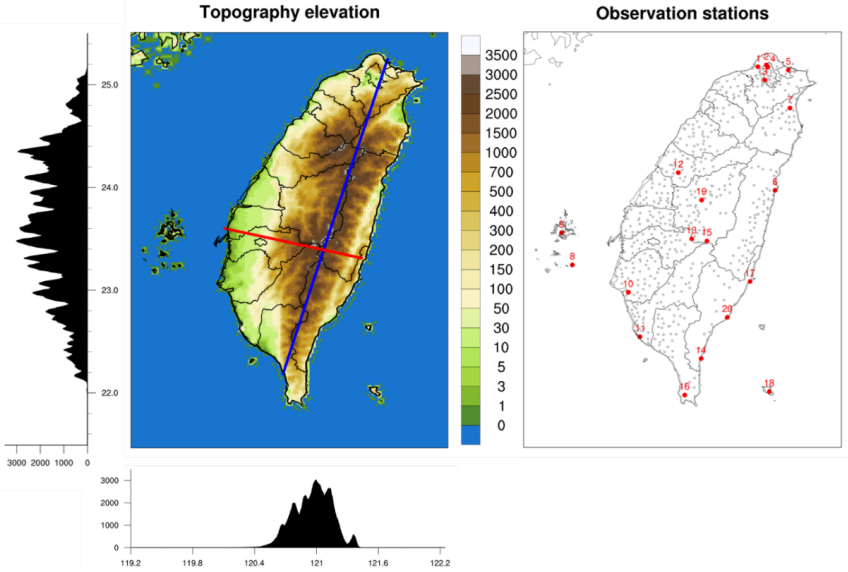

Figure 1. (left) Topography of Taiwan with 2-km resolution, the left and bottom panels are the profiles of altitude (meters) along the blue and red lines. (right) locations of the (red dots) weather stations and (gray dots) automatic rain gauges of Taiwan's Central Weather Administration (CWA hereafter)

https://doi.org/10.5194/essd-2026-242
Preprint. Discussion started: 20 April 2026

2. Method and data

2.1 Model configurations

The dynamical downscaling was conducted over two nested domains (as shown in Figure 2) using WRF (version 3.8.1, Skamarock and Klemp, 2008). The horizontal resolutions of the entire and inner domains are 10 km (250 × 250 grid cells) and 2 km (220 × 280 grid cells), respectively. The use of the two domains with varying resolutions is to simultaneously fulfill the needs of high resolution for climate change application and to allow the evaluation and analysis of synoptic weather systems that support the former. The model has 52-layer vertical sigma coordinates with the top layer of the atmosphere being 30 hPa. As for the terrain elevation, Global Multi-Resolution Terrain Elevation Data developed by the U.S. Geological Survey (USGS) and the U.S. National Geospatial-Intelligence Agency of approximate 1-km resolution (Danielson and Gesch, 2011) was applied in the model after regridding. As shown in Figure 1, after preprocessing, Taiwan's mountain ranges (about 1500-3000 m) and valleys can be well resolved with 2-km resolution, adequately representing the complexity of topography.

Regarding the physical parameterizations, the Goddard microphysics scheme and the Kain–Fritsch scheme were chosen as the cloud microphysics scheme and the cumulus parameterization scheme (Kain and Fritsch, 1990; Kain, 2004; Lim et al., 2010), respectively. These schemes were implemented only in the 10-km domain. The planetary boundary layer parameterization is the Yonsei University scheme (Hong and Pan, 1996), and the longwave and shortwave radiation parameterization is the Rapid Radiative Transfer Model scheme (Mlawer et al., 1997; Iacono et al., 2008). The parameterization of the surface layer and the land surface are the Monin–Obukhov scheme (Monin and Obukhov, 1954) and the Noah Land Surface Model (Chen and Dudhia, 2001), respectively.

https://doi.org/10.5194/essd-2026-242
Preprint. Discussion started: 20 April 2026

Open Access Earth System Science Data Discussions

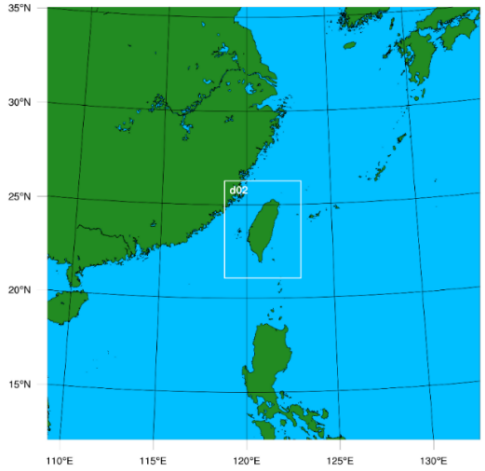

Figure 2. The two-layer nested domains used in the WRF simulation: the entire and the inner (d02, the white box) domains of 10-km and 2-km resolutions, respectively

Land use and land cover changes have considerable effects on regional climate (Lin et al., 2008; Cheng et al., 2013). For instance, urban areas are generally warmer than the surrounding areas due to the heat island effect (He et al., 2021). Since urbanization occurred in Taiwan in the past decades, it is important to realistically reflect the land cover changes when modeling regional-scale climate change. As such, the frequently used land cover data that was integrated using Taiwan's historical maps and satellite images (Chen et al., 2019) was applied in this study. Specifically, the land cover maps of 1982, 1995, 2000 and 2015 have been used in simulations to respectively represent the land use conditions during the following intervals: 1979-1988, 1989-1997, 1998-2007 and 2008-2018. As shown in Figure 3, the distribution of land uses notably vary in the four years, particularly the expansion of city/urban (i.e., red grids) and the decreases in cropland and pasture regions (i.e., gray and orange grids).

https://doi.org/10.5194/essd-2026-242
Preprint. Discussion started: 20 April 2026

Open Access Earth System Science Data Discussions

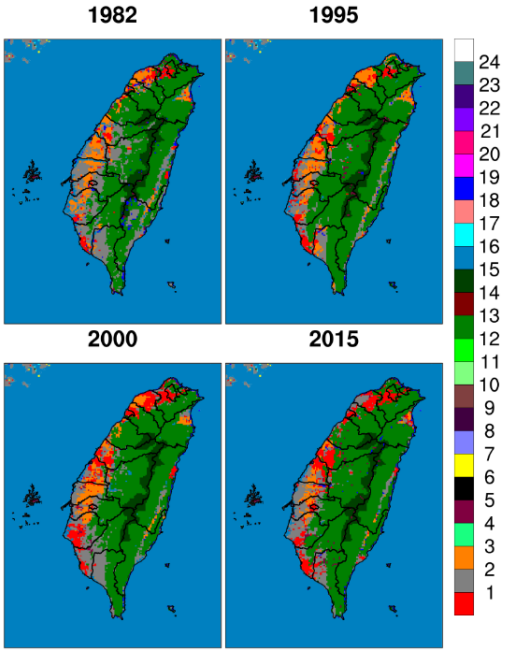

Figure 3. Distributions of the land use types in Taiwan in the years 1982, 1995, 2000 and 2015 (the USGS 24 categories of WRF can be found in Table S2)

2.2 Reforecasting data and method

With the model configuration described in Section 2.1, the re-forecast has then been conducted using ERA5's hourly atmospheric variables for the period from 1980 to 2019 (Hersbach et al., 2018a, 2018b, 2020). To avoid accumulating biases through the long-term numerical modeling, regularly integrating short-term simulations, or applying nudging has been used in dynamical downscaling (Lo et al., 2008).

Figure 4 shows the flowchart of re-forecasting steps described as below. Firstly, a one-month spin-up was conducted in the first simulation before blending with ERA5 data. After that, sequential 12-hour modeling was then re-initialized every 6 hours. Since only the second 6-hour results were preserved (i.e., the first 6-hour was considered as spin-up), the hours of 00, 06, 12 and 18Z in ERA5 were blended in each 12-hour modeling. This approach is to minimize the biases accumulated through the simulation. Lastly, all the preserved 6-hour results were then combined to form the long-term climate data set.

To ensure that the model rapidly achieved equilibrium in the initial period of the simulation, the digital filter initialization method introduced by Lynch and Huang (1992) was performed.

https://doi.org/10.5194/essd-2026-242
Preprint. Discussion started: 20 April 2026

Open Access Earth System Science Data Discussions

Additionally, a blending method was applied in this study to keep small-scale features simulated by WRF from being erased by the ERA5-driven re-initializations. Thus, following the same strategy developed by Yang (2005), the circulations with scales above 1000 km (mainly from ERA5) were combined with the small-scale WRF-forced perturbations. Moreover, the post-blending results were then used as the initial states of the subsequent 12-hour simulations. After combining all the second 6-hour reforecasts, this newly reconstructed climate data set, the Taiwan ReAnalysis Downscaling data (TReAD hereafter), was then evaluated as described in the next section.

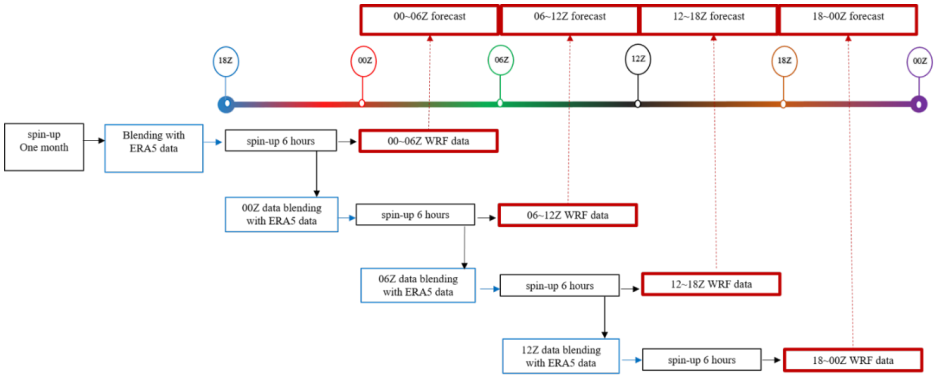

Figure 4. Flowchart of the reforecasting process applied in the WRF simulation

2.3 Observation data for evaluation

To evaluate TReAD, CWA's station observation data was compared with the closest grid cell of TReAD of the original resolution. As shown in Figure 1 (left panel), there are 17 stations on the plain and 5 on the mountainous regions, namely Anbu, Zhuzihu, Alishan, Yushan, Sunmoonlake (see Table S1 for the details of the 22 stations including longitude, latitude and elevations). It is worthy mentioning that the elevations of the 5 mountainous stations range from 607 to 3844 m that is valuable when evaluating a region with highly-varying topography.

Since the elevations of the point-based CWA observation data are different from that of TReAD that represents a grid-cell average, the TReAD temperatures have been adjusted using a lapse rate of 0.65°C per 100 m before comparison. Moreover, the grid cells in TReAD that are closest to the coordinate of CWA's stations were used for comparison.

One of the advantages of TReAD is the spatial distribution of the reconstruction that is highly demanding for the climate change application, thus the observation-based gridded data set from the

https://doi.org/10.5194/essd-2026-242
Preprint. Discussion started: 20 April 2026

Open Access Earth System Science Data Discussions

Taiwan Climate Change Projection Information and Adaptation Knowledge Platform project (TCCIP) has been used to evaluate the results (Weng and Yang, 2018). In order to compare 2-km resolution TReAD with 1-km resolution TCCIP data set, an elevation adjustment has been applied to TReAD. In detail, to correct the biases induced by the grid-average elevation of TReAD when evaluating the simulated temperature, the elevation of the station which is closest to each grid cell has been used to adjust the temperature. After the elevation adjustment, TReAD was then re-gridded to 1 km with bilinear interpolation method.

Another important observational data set is the Himawari 8-derived shortwave radiation (Bessho et al., 2016). To compare the simulated radiation of TReAD, both station-based and satellite-derived CWA (i.e., available for the period from 2011 to 2018) data sets have been used. However, there is no radiation measurement for some stations in the early years of the period. Therefore, only the grid points of TReAD that the station measurements are available have been used for fair comparison.

https://doi.org/10.5194/essd-2026-242
Preprint. Discussion started: 20 April 2026

Open Access Earth System Science Data Discussions

3 Results and Discussion

3.1 2-m air temperature

The TReAD temperature data was firstly evaluated using CWA observations. To understand the overall performance (and its variability) of TReAD, the 40-year average correlation coefficients and Root Mean Square Errors (RMSEs) of daily temperatures between the elevation-adjusted TReAD and the CWA data were computed and shown in Figure 5.

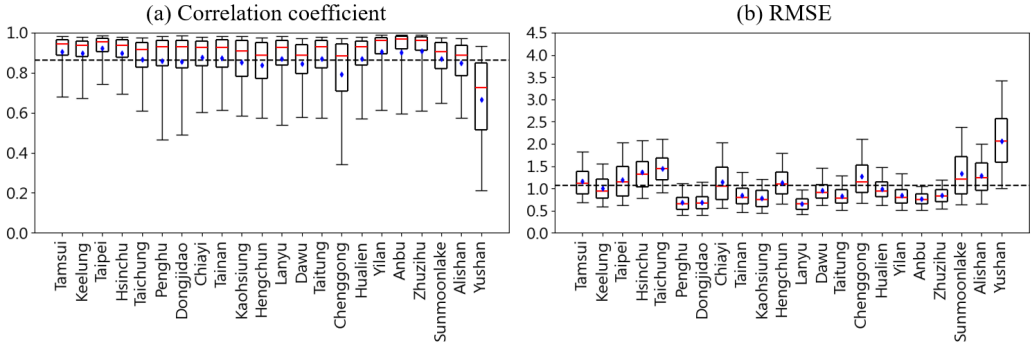

Figure 5. The average (a) correlation coefficients and (b) RMSEs (°C) of daily temperatures between the elevation-adjusted TReAD and the station-based CWA data for the period from 1980 to 2019. The dashed lines represent the average of all stations and the blue points and red lines in each boxplot indicate means and medians, respectively.

The result of the comparison between the point-based CWA and area-average TReAD temperatures is generally satisfactory for most of the stations. The (interquartile of) correlation coefficients are above 0.7 for 90% of the stations with the average of 0.86. Moreover, most (interquartile of) RMSEs fall in between 0.5-1.5. However, the performances of the mountainous stations are relatively lower. For instance, the correlation coefficients and RMSEs of the Yushan station range between 0.5-0.8 and 1.5-2.5, respectively. This indicates the difficulty of modeling grid cells with high altitudes (e.g., above 3000 m). Nevertheless, the other two high-land stations (Alishan and Sunmoonlake with elevations above 2400 and 1000 m) attain the results that are comparable with the values of the flat plain.

https://doi.org/10.5194/essd-2026-242
Preprint. Discussion started: 20 April 2026

Open Access Earth System Science Data Discussions

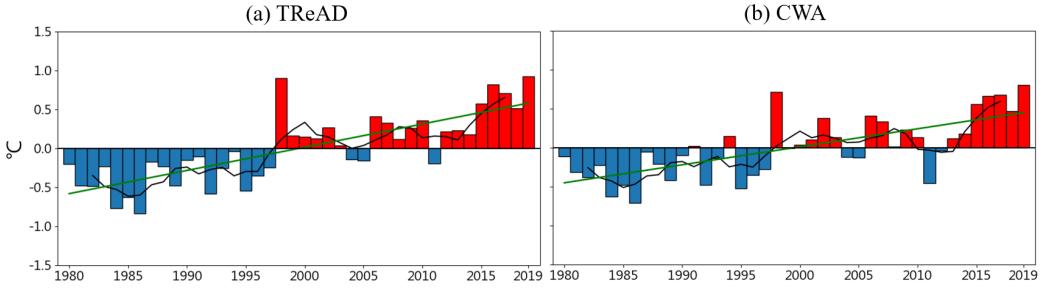

Figure 6. Anomalies of annual mean temperature for (a) TReAD and (b) CWA from 1980 to 2019. The red and blue bars represent hotter and cooler years when compared to the average of the entire period. The black time series indicate 5-year moving averages of annual mean temperatures. The green lines are the 40-year trend (linear regression).

In addition to the correlation coefficients and RMSEs, the mean biases were also evaluated (see Figure 5) to better understand the feature of differences (TReAD minus CWA). In general, TReAD tends to underestimate temperatures in those mountainous locations such as Yushan, Alisan and Sunmoonlake by 1.2-1.9℃ and overestimate temperatures in the other stations like Taichung and Taipei by 0.8-1.2℃. What's more, the long-term trend and the relevant interannual variability are important and have been analyzed (see Figure S1a), it is found that there are similarly increasing trends of temperature for both data sets from 1980 to 2019. The interannual variabilities are analogous as well. This long-term trend remains for both datasets even when evaluating the mountainous and plain areas separately (not shown here). Therefore, TReAD well reproduces the observed long-term warming trend and the variability in Taiwan, including the sharp up-and-down occurring around 1998.

The correlation coefficients of monthly temperatures were further examined in four seasons: 0.92, 0.73, 0.86 and 0.95 in spring, summer, fall and winter. The relatively lower correlations in summer could be mainly due to the fact that there are more small-scale convective systems during summer.

https://doi.org/10.5194/essd-2026-242
Preprint. Discussion started: 20 April 2026

Open Access Earth System Science Data Discussions

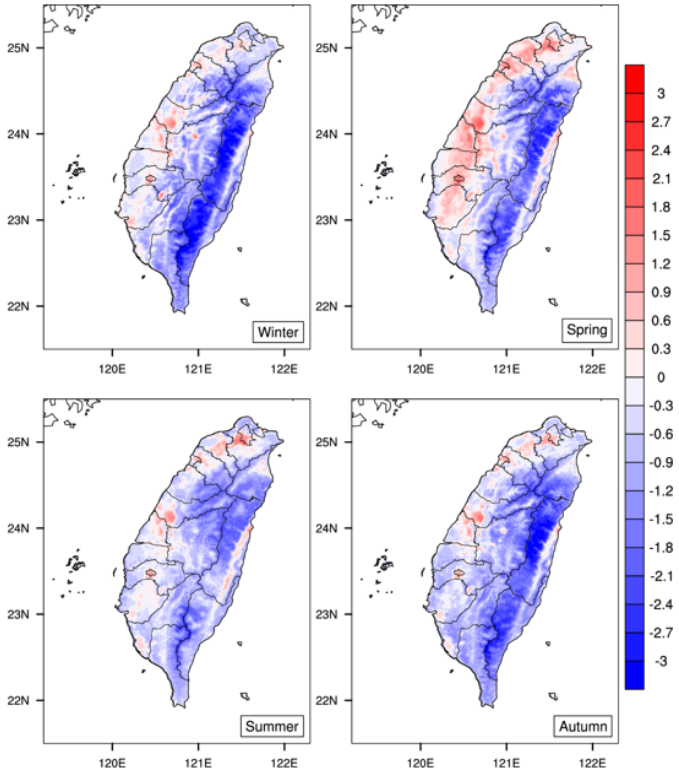

Figure 7. 40-year mean biases (TReAD minus TCCIP) of daily temperatures in four seasons for the period from 1980 to 2019. The blue (red) grid cells represent that TReAD shows cool (warm) biases.

Figure 7 shows the seasonal patterns of mean biases of daily temperatures between TReAD and TCCIP data sets. Overall, the 40-year mean biases vary with Taiwan's terrain. Specifically, TReAD shows negative anomalies (cool biases) in the mountainous regions in all the four seasons and a relatively weak overestimation (warm biases) on the plain mainly in spring. As such, attention should be drawn from the users who are interested in the long-term changes in the major cities and in the mountainous areas.

To understand the differences of the long-term trend and interannual variabilities of temperatures among TReAD, CWA and TCCIP, the time series of annual mean of daily temperatures (including mean, maximum and minimum) for the entire 40 years (1980-2018) are shown in Figure 8. It is shown that the observed 40-year warming trend and the interannual variability of all three temperatures are realistically reproduced by TReAD (and TCCIP) when comparing with CWA. However, TReAD and TCCIP show varying biases for the maximum and minimum temperatures. Specifically, TReAD underestimates the daily maximum temperatures by around 1°C and slightly overestimates daily

https://doi.org/10.5194/essd-2026-242
Preprint. Discussion started: 20 April 2026

minimum temperatures by around 0.2℃ (see the red and black lines in Figure 8b and 8c). It is worthwhile to mention here that TReAD could effectively capture the peaks (e.g., in 1998) seen in the time series of observations for the daily mean, maximum and minimum temperatures.

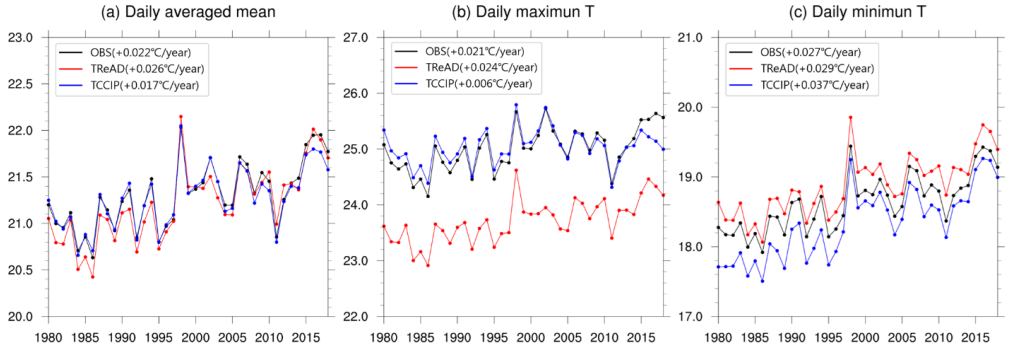

Figure 8. Annual time series of daily (a) mean, (b) maximum and (c) minimum temperatures of Taiwan as a whole for the period from 1980 to 2018. The black, red and blue lines represent CWA, TReAD and TCCIP, respectively. The slopes of the linear trends of each time series are given in the legends.

3.2 Precipitation

As shown in Figure 9, TReAD shows a reasonable performance for precipitation although there are relatively lower long-term correlation coefficients and higher RMSEs when compared with temperature described in Section 3.1. The overall average of correlation coefficients is 0.59 and its seasonal variability ranges between 0.57-0.62 (not shown here). Furthermore, the correlation coefficients do not show a regional pattern i.e., the values are similar in both plain and mountainous areas. By contrast, there are higher RMSEs of TReAD's precipitation in mountainous stations than in the plain.

In terms of the interannual variability and long-term trend, Figure 10 shows the anomalies of annual precipitation for both TReAD and CWA. It is shown that TReAD well reproduces the observed interannual variability of precipitation as well as the 40-year increasing trend. In particular, the two peaks around the years 2000 and 2006 can be seen in both time-series.

https://doi.org/10.5194/essd-2026-242
Preprint. Discussion started: 20 April 2026

Open Access Earth System Science Data Discussions

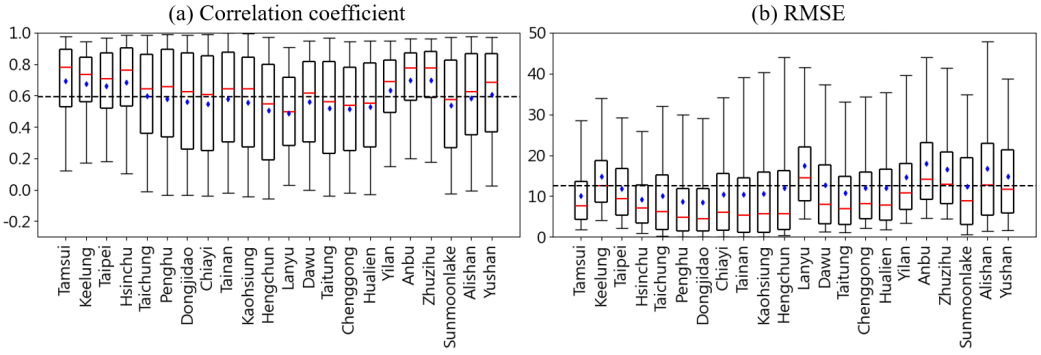

Figure 9. The average (a) correlation coefficients and (b) RMSEs (mm) of precipitation between TReAD and CWA data sets for the period from 1980 to 2019. The dashed lines represent the average of all stations and the blue points and red lines in each boxplot indicate means and medians, respectively.

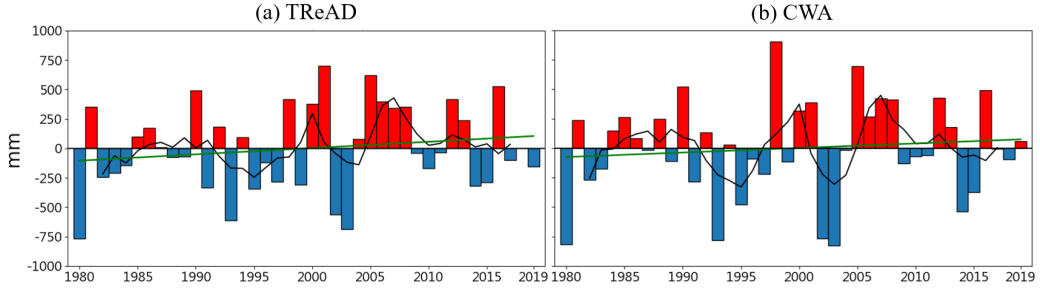

Figure 10. Anomalies of annual precipitation for (a) TReAD and (b) CWA from 1980 to 2019. The red and blue bars represent wet and dry years when compared to the average of the entire period, respectively. The black time series indicates 5-year moving averages of precipitation. The green lines are the 40-year trendline of linear regression.

To evaluate the variabilities of the spatial distribution of seasonal precipitation, TReAD is compared with TCCIP for four seasons (i.e., spring, summer, autumn and winter). As shown in Figure 11, the key characteristics of spatial pattern of the seasonal precipitation of the TCCIP data set can be well reproduced by TReAD. For example, the maximum precipitation observed in the north and northeastern areas in winter and spring seasons can be realistically simulated. In summer, the rainfall pattern is influenced by the prevailing southwestern wind and the terrain effect. Thus, the heavy rainfall simulated by TReAD could be seen over the southwestern Taiwan as well as along the windward side of the mountain located in the center (see Figure 1). In autumn, the northeastern monsoon brings the moisture to the north and northeastern areas of Taiwan where TReAD reasonably reproduced the pattern. However, Figure 11 (bottom row) shows that TReAD basically overestimates

https://doi.org/10.5194/essd-2026-242
Preprint. Discussion started: 20 April 2026

precipitation in Taiwan, particularly over mountainous regions in summer and autumn when compared with TCCIP. Since the observation stations in the mountainous region are relatively fewer and sparsely distributed, there could be higher biases for the reconstructed TCCIP precipitation.

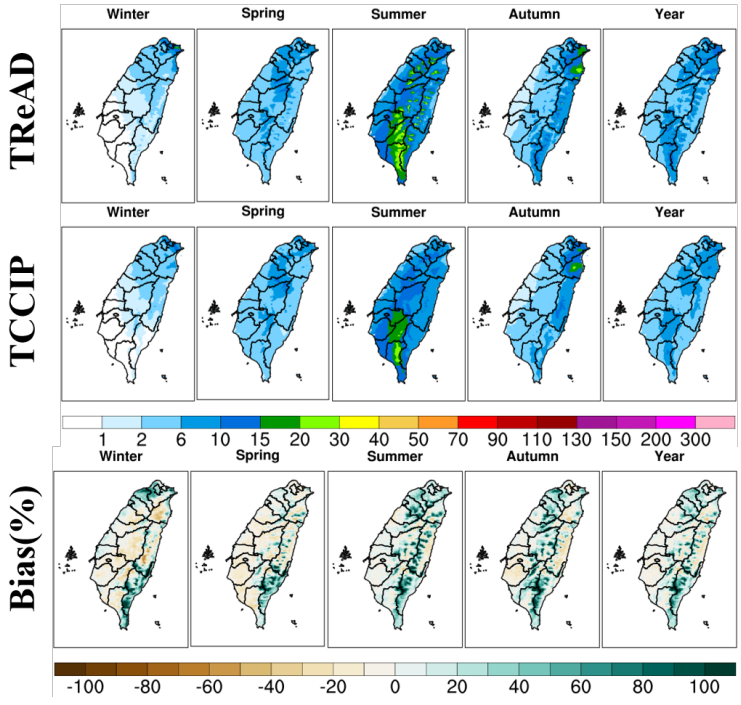

Figure 11. 40-year average of seasonal and annual precipitation for (top row) TReAD, (mid row) TCCIP and (bottom row) the biases (TReAD minus CWA) for the period from 1980 to 2018. Seasons are indicated as the title of each column: winter, spring, summer and autumn and the yearly mean (from left to right).

To be better applied to climate change impact and adaptation fields, the capability of reproducing extreme precipitation events is important and has been evaluated by assessing the typhoon Morakot that resulted in severe flooding events across Taiwan in 2009. As shown in Figure 12, the spatial patterns of the observed (TCCIP) daily precipitation throughout the four days are well simulated by TReAD. It is clear that TReAD reproduced the 4-day evolution while slightly underestimating the precipitation in the mountain areas that could be seen in the total and average precipitation shown in the two right-end columns.

https://doi.org/10.5194/essd-2026-242
Preprint. Discussion started: 20 April 2026

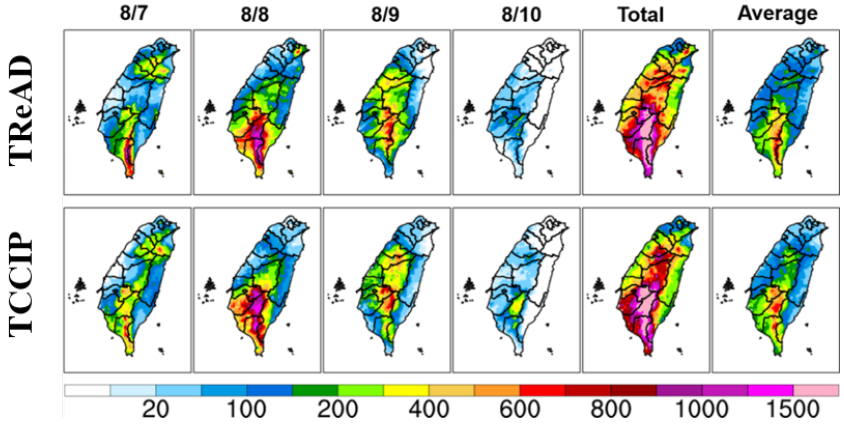

Figure 12. Variabilities of precipitation of TReAD and TCCIP for the typhoon Morakot in 2009

3.3 Atmospheric pressure

In addition to the effect of Taiwan's complex topography, the atmospheric pressure is significantly affected by strong weather systems such as typhoons which are common in summertime Taiwan. Figure 13 shows the correlation coefficients and RMSEs of atmospheric pressure of TReAD against CWA for the period from 1980 to 2019. Overall, TReAD performs well in terms of both metrics: correlation coefficients are well above 0.93 and RMSEs fall below 2 hPa for the majority of the CWA stations. However, the correlation coefficients are slightly lower for mountainous stations such as Yushan, Alishan and Sunmoonlake. The biases might come from the remaining discrepancies of elevation between the model grids and the stations even if the former was adjusted. Additionally, Lanyu also attains lower correlation coefficients possibly because that model fails to capture its exact location due to the small size (around 45 km^2).

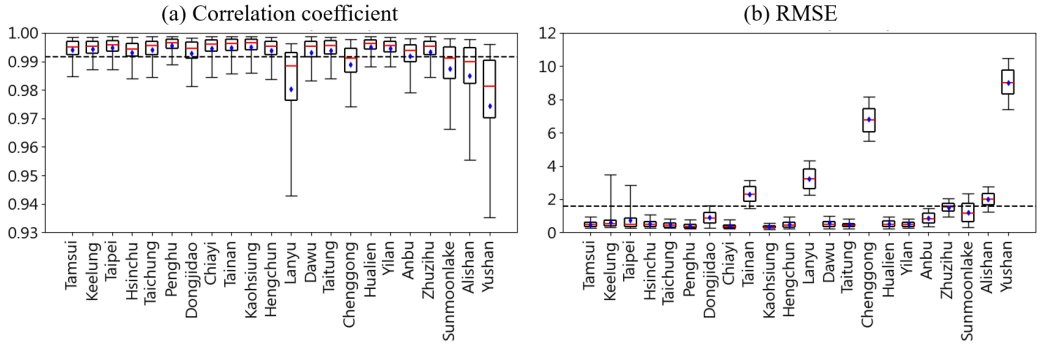

Figure 13. The average (a) correlation coefficients and (b) RMSEs (hPa) of atmospheric pressure between TReAD and CWA data sets for the period from 1980 to 2019. The dashed lines represent the average of all stations and the blue points and red lines in each boxplot indicate means and

https://doi.org/10.5194/essd-2026-242
Preprint. Discussion started: 20 April 2026

medians, respectively.

To further examine TReAD's performance of temporal variability of air pressure, four stations for both plain and mountainous areas are selected: Taipei, Taichung, Dawu, and Yushan. The time series of daily atmospheric pressure of TReAD and CWA in September 2001 (during two typhoon events (Nari of 16-19 and Lekima of 26-28) are shown in Figure 14. Generally, TReAD well simulated the variabilities of atmospheric pressure for all four stations. Particularly, the two drops induced by typhoons have been reasonably replicated by TReAD. However, TReAD underestimated the air pressure in Yushan station by about 12 hPa possibly due to the lower intensity of the simulated typhoon.

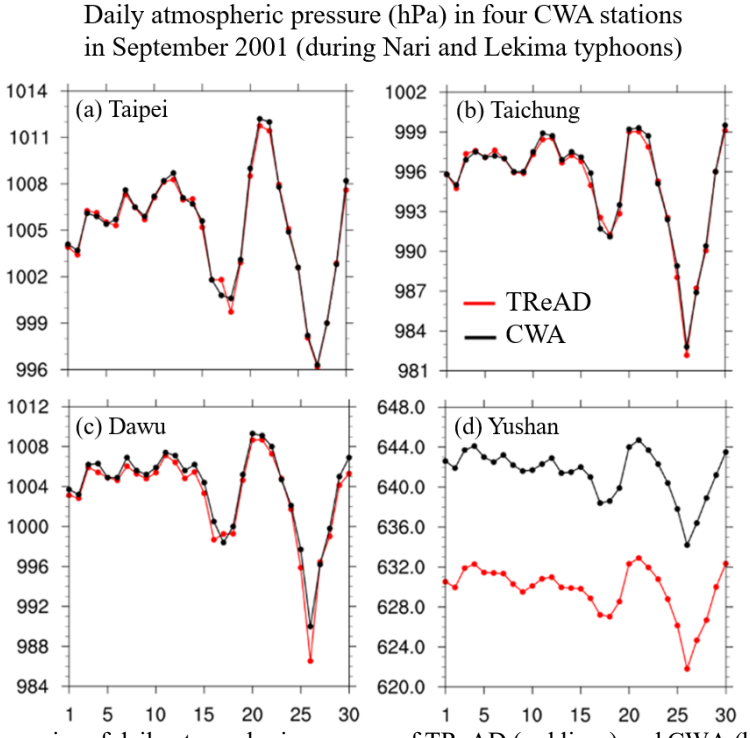

Figure 14. Time series of daily atmospheric pressure of TReAD (red lines) and CWA (black lines) in (a) Taipei, (b) Taichung, (c) Dawu and (d) Yushan stations in September 2001. Typhoons Nari and Lekima hit Taiwan between 16-19 and 26-28 September, respectively.

3.4 Shortwave radiation

Radiation is one of the most important climate factors for impact studies such as the urban heat island (UHI) field (Ulpiani, 2021) because of its significant impact on surface temperature through the

https://doi.org/10.5194/essd-2026-242
Preprint. Discussion started: 20 April 2026

Open Access Earth System Science Data Discussions

energy budget at regional scale. The 40-year averages of correlation coefficients and RMSE of shortwave radiation between TReAD and CWA data sets for the period from 1980 to 2019 are assessed and shown in Figure 15. The medians of correlation coefficients are often above 0.6 with the all-station average of 0.70 and the medians of RMSEs range between 6-10 (MJ m^{-2}). No regional characteristics can be found for both metrics. As for the interannual variability of the radiation anomalies for the same period as shown in Figure 16, the variability of TReAD ranged between ±1 which is smaller than that of CWA. The performance of TReAD on the long-term variability of radiation is poor although the two positive anomalies around the years 2004 and 2010 are relatively comparable.

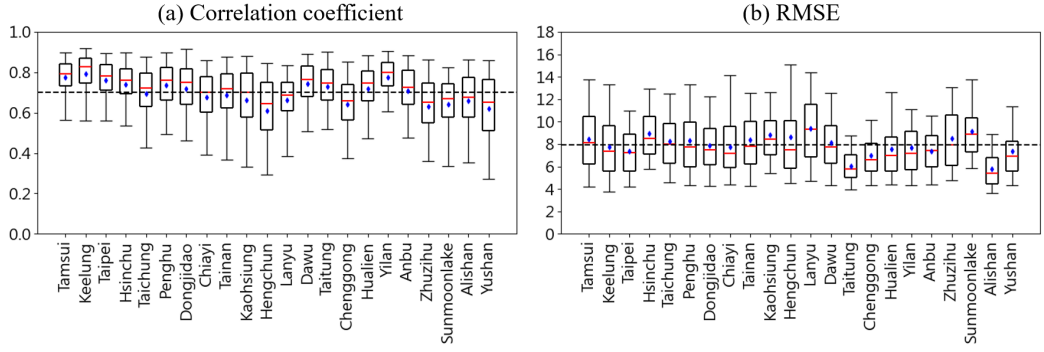

Figure 15. The average (a) correlation coefficients and (b) RMSEs (MJ m^{-2}) of shortwave radiation between TReAD and CWA data sets for the period from 1980 to 2019. The dashed lines represent the average of all stations and the blue points and red lines in each boxplot indicate means and medians, respectively.

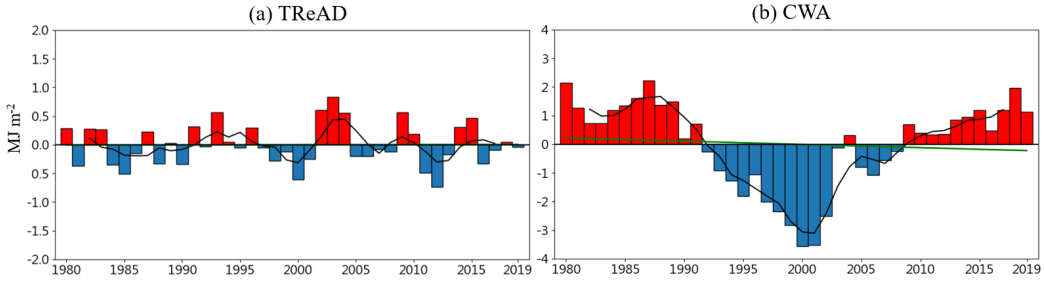

Figure 16. Anomalies of annual shortwave radiation for (a) TReAD and (b) CWA from 1980 to 2019. The red and blue bars represent positive and negative years when compared to the average of the entire period, respectively. The black time series indicates 5-year moving averages of shortwave radiation. The green lines are the 40-year trendline of linear regression.

To understand the improvement of the simulated radiation, from ERA5 to TReAD, the daily radiation

https://doi.org/10.5194/essd-2026-242
Preprint. Discussion started: 20 April 2026

datasets have been evaluated by comparing with CWA for the period from 2011 to 2018. As shown in Figure 17, the high-resolution TReAD could well resolve the observed spatial pattern of radiation when compared with the 25-km resolution ERA5 although the former tends to show positive biases across Taiwan. Moreover, the enhancement of performance can be seen by the increased correlation coefficients from ERA5 to TReAD throughout the seasons of a year, particularly in summer and autumn, as shown in the corresponding panels of Figure 17. The improved and detailed information of radiation is valuable for the subsequent impact study. For instance, TReAD could be a solution for the inability of provision of the long-term historical radiation by short-term satellite-derived observations and then provide more opportunities for the heat island field by supplying historical high spatial resolution radiation data.

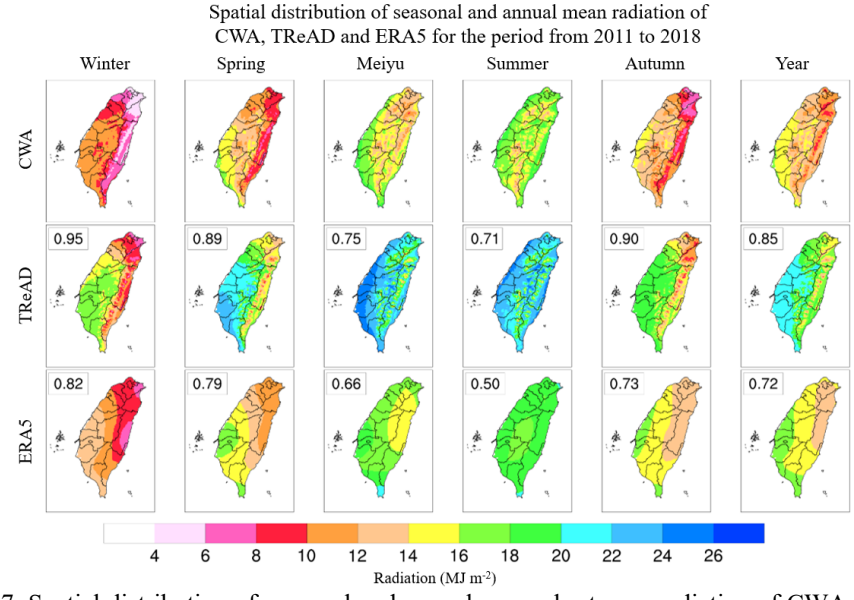

Figure 17. Spatial distribution of seasonal and annual mean shortwave radiation of CWA (satellite-derived), TReAD and ERA5 for the period from 2011 to 2018. The correlation coefficients of simulated radiation against CWA are shown at the top-left corners of the panels of TReAD and ERA5.

Since radiation is significantly affected by the cloud-related weather systems (e.g., convective precipitation or typhoons), the simulated daily cumulative radiation has been further assessed by comparing it with CWA data sets (both station-based and Himawari-8 derived) for four observation stations (i.e., Taipei, Taichung, Dawu, and Kaohsiung) as shown in Figure 18. Overall, TReAD can capture the daily variabilities of radiation for all four stations and in the four months even though the aforementioned biases remain. Furthermore, it is worthy mentioning that TReAD well simulated the drop of radiation on 7-9 July that typhoon Nepartak hit Taiwan in 2016.

https://doi.org/10.5194/essd-2026-242
Preprint. Discussion started: 20 April 2026

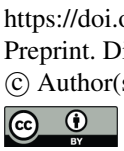

Open Access Earth System Science Data Discussions

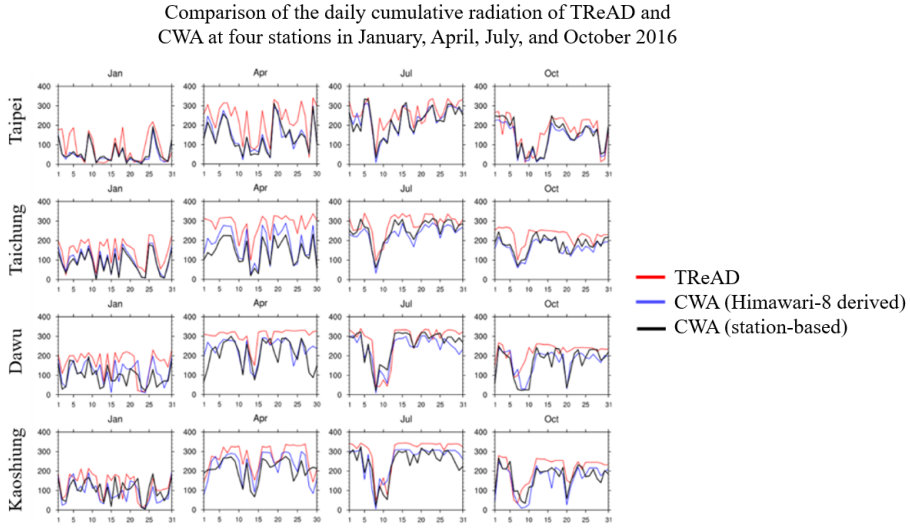

Figure 18. Daily cumulative shortwave radiation (W m^{-2}) of (red) TReAD, (blue) CWA (Himawari-8 derived) and CWA (station-based) at Taipei, Taichung, Dawu, and Kaohsiung observation stations (row-wise) in January, April, July, and October (column-wise) 2016

3.5 Wind velocity

Wind velocity is an important climatic factor for the application sectors. On the one hand, it has been linked to the cooling of air temperatures in the urban areas (Memon et al., 2010) and can be an efficient solution for the UHI issues (Wang et al., 2024). The wind extreme events (such as wind gusts induced by typhoons) can, on the other hand, cause damage to vegetation in the ecological sector (Wang and Huang, 2023). However, the measurements of wind velocity are much sparsely distributed than temperature and precipitation. Thus, interpolation methods have been frequently applied to estimate it over the regions without observations (Luo et al., 2008).

To evaluate TReAD's wind velocity, it has been compared to the station-based CWA and the original ERA5 data sets. Figure 19 shows the average correlation coefficients and RMSEs of daily wind velocity of TReAD against CWA data for the period from 1980 to 2019. The all-station average of correlation coefficients is 0.69 and the majority of plain stations attain values above 0.6 while mountainous stations show a relatively poor performance (around 0.3-0.5) and larger differences among stations. In terms of RMSEs, most stations attain values well below the average (the dashed line) but there are larger biases for some stations like mountainous regions (Yushan) and remote islands (Lanyu and Penghu) probably due to the imprecise information on terrain (including land-sea

https://doi.org/10.5194/essd-2026-242
Preprint. Discussion started: 20 April 2026

intersections).

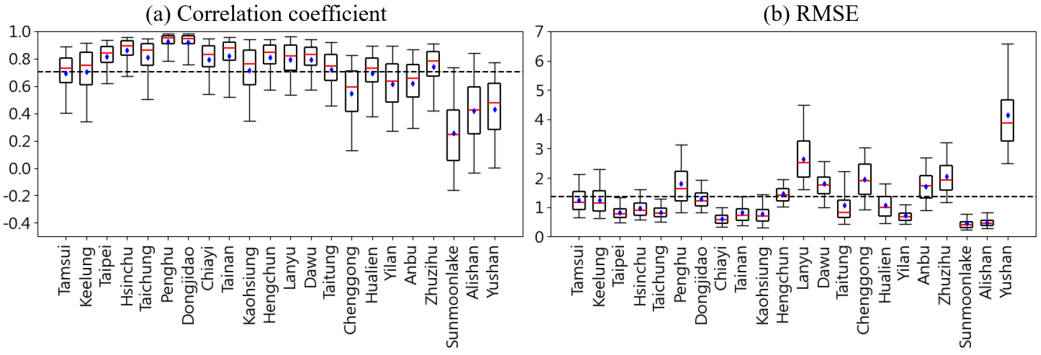

Figure 19. The average (a) correlation coefficients and (b) RMSEs (m s^{-1}) of daily wind velocity between TReAD and CWA data sets for the period from 1980 to 2019. The dashed lines represent the average of all stations and the blue points and red lines in each boxplot indicate means and medians, respectively.

The 40-year long term trend of wind velocity has also been evaluated by comparing the anomalies of wind velocity against CWA data as shown in Figure 20. The wind velocity simulated by TReAD shows a decreasing trend as that of CWA during the entire period although the performance is relatively poor in the first half of the period. Specifically, TReAD's annual anomalies are much smaller, particularly during the first two decades.

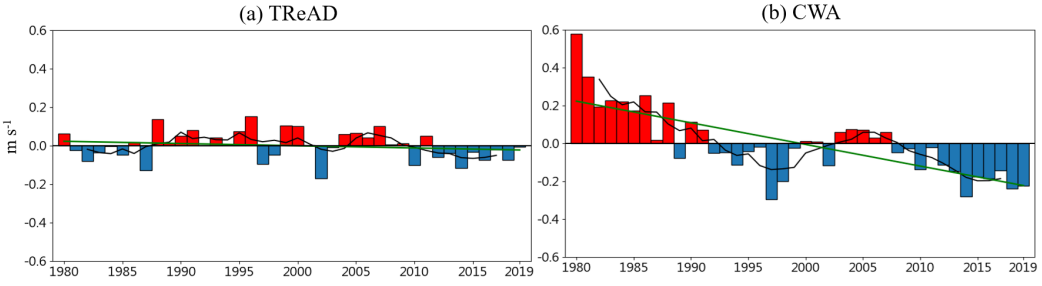

Figure 20. Anomalies of wind velocity for (a) TReAD and (b) CWA from 1980 to 2019. The red and blue bars represent positive and negative years when compared to the average of the entire period, respectively. The black time series indicates 5-year moving averages of wind velocity. The green lines are the 40-year trendline of linear regression.

https://doi.org/10.5194/essd-2026-242
Preprint. Discussion started: 20 April 2026

Open Access Earth System Science Data Discussions

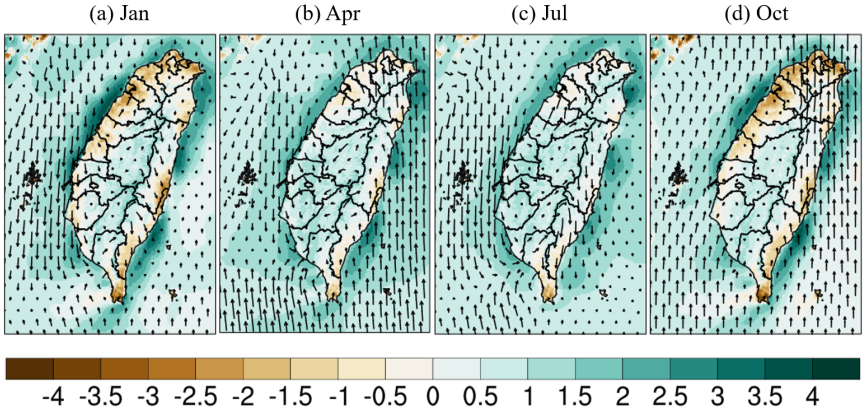

Figure 21. Differences of the average wind velocity between TReAD and ERA5 (TReAD minus ERA5) for (a) January, (b) April, (c) July and (d) October of the entire period

To understand the improvement of the spatial pattern of wind velocity simulated by TReAD, it has been compared with ERA5 for January, April, July and October of the 40-year period as shown in Figure 21. Firstly, TReAD shows improved wind velocities particularly along the coastline. Since the low horizontal resolution of ERA5 resulted in a significantly imprecise land fraction for Taiwan (see Figure S2), the induced incorrect roughness then led to biases in wind velocity i.e., overestimate/underestimate in land/oceanic portion of the coastal grid cells. Figure 21 shows that TReAD's wind velocities are smaller (higher) in the land (oceanic) areas along the coastline when compared to that of ERA5 mainly due to the improved details of land-sea distribution.

In terms of daily variability, TReAD and ERA5 have been assessed by comparing with CWA observations as shown in Figure 22. The comparison of daily wind velocities reveals that TReAD simulation shows an improvement i.e., refining the wind velocity of ERA5 at coastal stations like Dawu and Kaohsiung. For instance, the strong wind velocities overestimated by ERA5 for the Dawu station have been remarkably improved by TReAD, showing smaller biases against CWA particularly in January, July and October. Moreover, TReAD also shows improvement when ERA5 underestimated wind velocities. Taking Kaohsiung station as an example, the underestimated wind velocities by ERA5 in April, July and October have been enhanced by TReAD (closer red and black lines).

https://doi.org/10.5194/essd-2026-242
Preprint. Discussion started: 20 April 2026

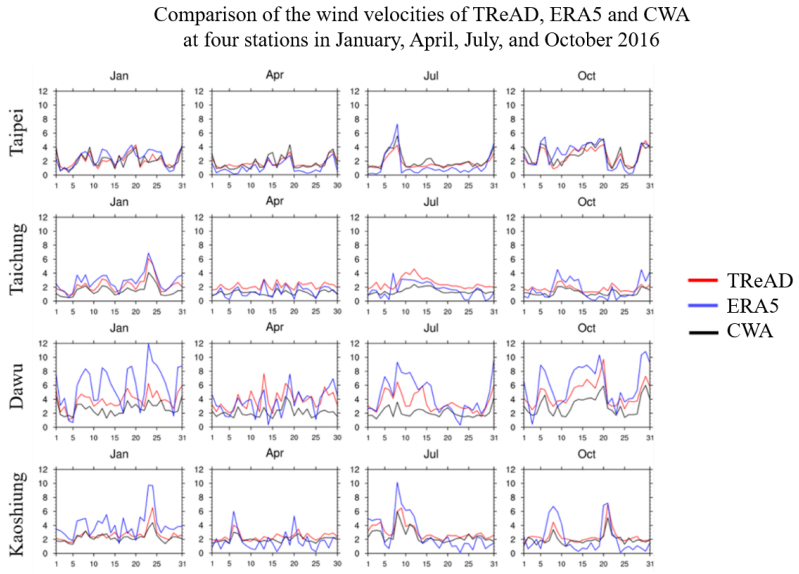

Figure 22. Daily wind velocities of TReAD (red), ERA5 (blue) and CWA (black) at four stations (i.e., Taipei, Taichung, Dawu and Kaohsiung) in January, April, July and October 2016

3.6 Relative humidity

Relative humidity is another important variable for climate change impact study. In addition to the aforementioned UHI field, the research on the impact of climate change on animal husbandry also highlights the importance of relative humidity e.g. the Temperature Humidity Index is frequently used as a hazard indicator for cows' industry (Liu et al., 2018). Therefore, TReAD aims to fill the gap by providing a 40-year gridded relative humidity data set for Taiwan which has not been available for decades.

Figure 23 shows the correlation coefficients and RMSEs of relative humidity between TReAD and CWA data sets. The all-station average of correlation coefficients is 0.73. The median of the majority of stations attains values above 0.7 while that of Hualien and Chenggong stations fall around 0.6. As for RMSEs, TReAD shows varying results with most stations ranging between 5% and 10% although there are higher RMSEs for some stations such as Yushan and Taichung stations. Since relative humidity is highly affected by temperature, thus the stations with higher biases of temperature often come with larger differences of relative humidity. On top of that, both land use/land cover and local weather systems like small-sale convective conditions and extreme events could simultaneously affect relative humidity, so the RMSEs show diverse performance across the stations.

https://doi.org/10.5194/essd-2026-242
Preprint. Discussion started: 20 April 2026

Open Access Earth System Science Data Discussions

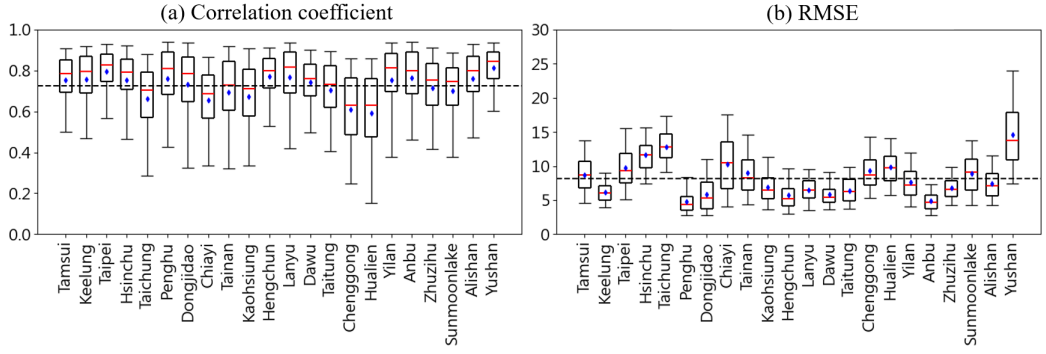

Figure 23. The average (a) correlation coefficients and (b) RMSEs (%) of relative humidity between TReAD and CWA data sets for the period from 1980 to 2019. The dashed lines represent the average of all stations and the blue points and red lines in each boxplot indicate means and medians, respectively.

As for the interannual variability of relative humidity and the 40-year long term trend, TReAD generally reproduced comparable results as CWA as shown in Figure 24. It can be seen that the decreasing trend has been well simulated and the change from positive anomalies to negative anomalies can be reasonably simulated when comparing the first and second half of the whole of 40 years.

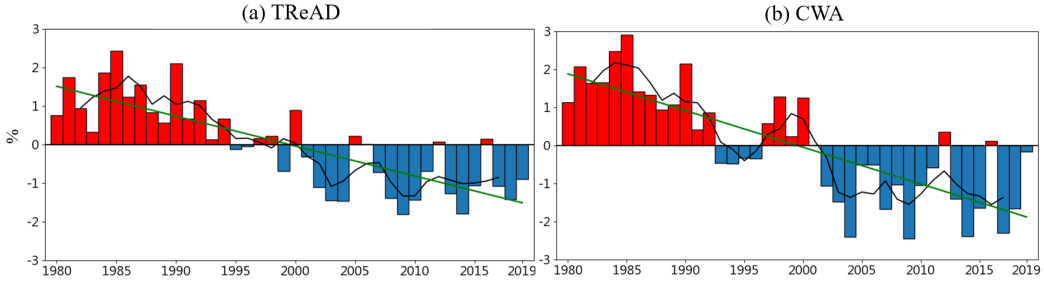

Figure 24. Anomalies of relative humidity for (a) TReAD and (b) CWA from 1980 to 2019. The red and blue bars represent positive and negative years when compared to the average of the entire period, respectively. The black time series indicates 5-year moving averages of relative humidity. The green lines are the 40-year trendline of linear regression.

As assessed for the other variables, Figure 25 shows the comparison of daily relative humidity between TReAD and CWA in January, April, July and October 2016 to understand its performance at a shorter timescale. Overall, the timeseries of relative humidity are comparable between two data sets in the four months in 2016. However, some discrepancies remain e.g., TReAD underestimated relative humidity for Taichung stations in all four months by up to around 20%. Nevertheless,

https://doi.org/10.5194/essd-2026-242
Preprint. Discussion started: 20 April 2026

509 TReAD's simulations closely follow the observed fluctuation at Kaohsiung station.
510

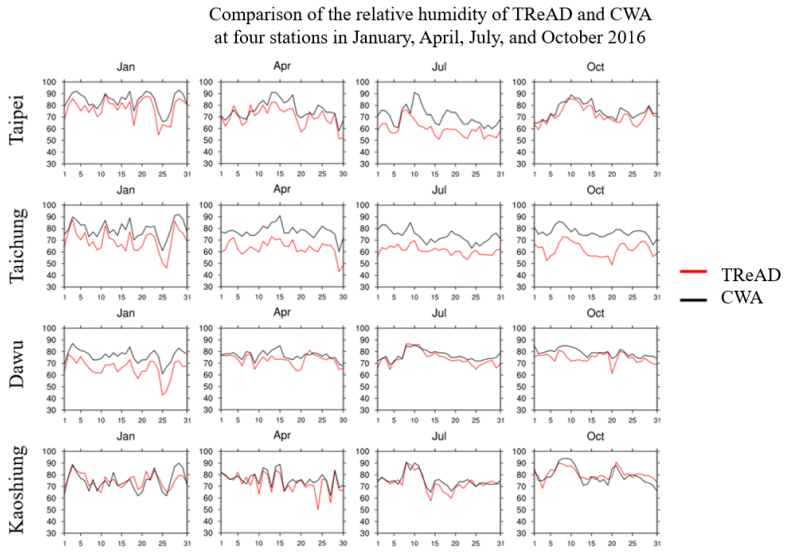

511
512 Figure 25. Daily relative humidity of TReAD (red) and CWA (black) at four stations (i.e., Taipei,
513 Taichung, Dawu and Kaohsiung) in January, April, July and October 2016

514 4 Data availability

515 TReAD data are available in the SciDM platform (Cheng et al., 2025, https://doi.org/10.30193/scidm-
516 rs-2576295). At this link, monthly values of mean temperature at 2 m height, near-surface relative
517 humidity, mean precipitation, accumulated downwelling shortwave flux, surface pressure and wind
518 speed at 10 m height for Taiwan at 2 km spatial resolution can be found. For the evaluation of our
519 TReAD data, different reference data were used, which are available online. Station data of Central
520 Weather Administration (CWA) of Taiwan are available at Climate Observation Data Inquire Service
521 (CODiS, https://codis.cwa.gov.tw/StationData). TCCIP's 5 km gridded observation datasets are
522 available for different domains, formats and temporal resolutions are available upon request via
523 project webpage (https://tccip.ncdr.nat.gov.tw/ds_03_mall.aspx).

524 5 Conclusion

525 There has been an increasing demand for long-term gridded observation data for the climate change
526 impact studies. Specifically, the quality and spatial resolution of the data are important particularly
527 over the regions with highly diverse topography such as Taiwan. There are three key challenges that
528 are focused in this work: firstly, the availability of observational data in the mountainous regions is

https://doi.org/10.5194/essd-2026-242
Preprint. Discussion started: 20 April 2026

still low; secondly, the accessible ECVs cannot fulfill the growing need for the impact studies; thirdly, a high temporal resolution gridded data set is important but still missing for the reconstruction, analysis and the multidisciplinary application of historical climate in Taiwan. Therefore, this study aims to re-forecast the detailed variability of a range of ECVs at a gridded basis across Taiwan from 1980 to 2019 by dynamically downscaling approach.

As for the data and method, the global ERA5 reanalysis product has been downscaled to Taiwan's domain (2-km resolution) by using WRF model along with the other global/local observational data sets including USGS's terrain elevation data at 1-km resolution and 500-m land use data of Taiwan (Chen et al., 2019). Furthermore, to minimize the biases that are accumulated through the 40-year simulation, we combined the second 6-hour reforecasts of all the 12-hour simulations and obtained the long-term reconstruction of historical climate in Taiwan (i.e., TReAD). In terms of evaluation, six ECVs (i.e., 2-m air temperature, precipitation, atmospheric pressure, shortwave radiation, wind velocity and relative humidity) have been quantitatively assessed to understand the biases of varying aspects of TReAD by compared with independent observations such as CWA's ground-based and satellite-derived data.

Overall, the result shows that all six ECVs of TReAD well capture the observed long-term characteristics of CWA's observational data. For example, the 40-year correlation coefficients for most variables are above 0.7 while precipitation attains slightly lower values around 0.6. Importantly, the observed warming trend can be seen in TReAD's temperature data as well. As for the differences of performance between the stations, both correlation coefficients and RMSEs generally show larger biases for the stations in the mountainous region such as Yushan.

When compared to the average of the entire 40 years, the observed interannual variabilities of the anomalies can be well reproduced by TReAD for all the ECVs except for wind velocity and shortwave radiation in which smaller anomalies were simulated. Nevertheless, TReAD effectively and significantly improves the spatial pattern and details of these two variables when compared to ERA5. Taking shortwave radiation as an example, the spatial correlation coefficients during summertime against CWA were increased from 0.5 to 0.72 as shown in Figure 17. Moreover, the spatial pattern seen in the observations, particularly in the central mountainous areas, have been well resolved in TReAD of 2-km resolution. On top of that, Figure 21 shows that TReAD constructively corrects the biases of ERA5's wind velocities along the coastline.

https://doi.org/10.5194/essd-2026-242
Preprint. Discussion started: 20 April 2026

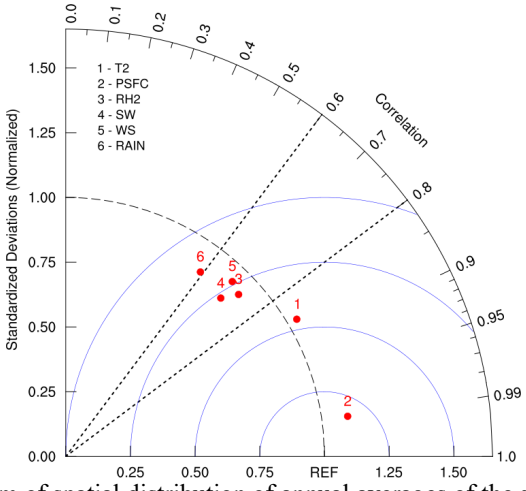

Figure 26. Taylor diagram of spatial distribution of annual averages of the six ECVs namely 2-m air temperature (1 - T2), atmospheric pressure (2 - PSFC), relative humidity (3 - RH2), shortwave radiation (4 - SW), wind velocity (5 - WS) and precipitation (6 - RAIN) against CWA dataset

Figure 26 shows the relative ranking of six ECVs in terms of the spatial distribution of annual averages. The variables attaining higher scores are atmospheric pressure and temperature followed by relative humidity and wind velocity. Specifically, the average correlation coefficients of the first two variables are above 0.8 and 0.9, respectively. However, both ECVs suffer larger biases for the mountainous regions. As for the latter two variables, improvements can be identified while discrepancies remain. As mentioned, overestimation/underestimation of wind velocities in the land/oceanic portions of grid cells have been improved given that the land-sea distribution was significantly enhanced. However, higher RMSEs can be seen in some remote islands such as Lanyu, in addition to the high-elevation locations (e.g., Yushan), probably due to imprecise terrain information.

The performance of shortwave radiation and precipitation is relatively lower. Both variables are highly affected by cloud-related weather systems such as typhoons and small-scale convective systems that frequently hit Taiwan, thus it indicates that the intensity or location of such systems might not be precisely simulated by WRF. As such, these two ECVs should be used with cautions and may need further correction. Despite that, the observed seasonal and annual spatial distribution of precipitation can be reasonably reproduced (see Figure 11) with wet biases mainly over the eastern side of the central mountain ranges. Additionally, the precipitation variability of typhoon Morakot in 2009 can be fairly reconstructed (see Figure 12). Furthermore, the long-term trend of annual precipitation anomalies was realistically simulated for the entire period.

https://doi.org/10.5194/essd-2026-242
Preprint. Discussion started: 20 April 2026

588
589 To sum up, the newly reconstructed TReAD data set is the first long-term gridded historical climate
590 data with high spatio-temporal resolution for Taiwan. A range of ECVs, including those that were
591 inaccessible from traditional observation data, have been validated using station-based and satellite-
592 derived data sets and can now be applied to the subsequent climate-related impact research. This
593 paper shows that dynamical downscaling can be a powerful tool to rebuild small-scale weather
594 patterns such as typhoons over the regions with high-rising mountains like Taiwan. The possibilities
595 of the future works followed include the validation of the variables at upper level of atmosphere,
596 reconstruction of the historical climate further backward with longer ERA5, etc. More importantly,
597 climate change impact studies are welcome to use TReAD which has been accessible upon request.

598 ## Acknowledgements

599 This work was supported by Taiwan Climate Change Projection and Information Platform Project
600 (TCCIP) programme funded by the Ministry of Science and Technology of Taiwan (MOST 107-
601 2621-M865-001). The ERA5 data set was downloaded from the Climate Data Store (CDS) of
602 Copernicus Climate Change Service (Hersbach et al., 2018a, 2018b).
603

https://doi.org/10.5194/essd-2026-242
Preprint. Discussion started: 20 April 2026

References

Bessho, K., Date, K., Hayashi, M., Ikeda, A., Imai, T., Inoue, H., ... & Yoshida, R. (2016). An introduction to Himawari-8/9—Japan's new-generation geostationary meteorological satellites. Journal of the Meteorological Society of Japan. Ser. II, 94(2), 151-183. https://doi.org/10.2151/jmsj.2016-009

Chen, T. C., Wang, S. Y., & Yen, M. C. (2007). Enhancement of afternoon thunderstorm activity by urbanization in a valley: Taipei. Journal of Applied Meteorology and Climatology, 46(9), 1324-1340. https://doi.org/10.1175/JAM2526.1

Cheng, A. R., Lee, T. H., Ku, H. I., & Chen, Y. W. (2016). Quality control program for real-time hourly temperature observation in Taiwan. Journal of Atmospheric and Oceanic Technology, 33(5), 953-976. https://doi.org/10.1175/JTECH-D-15-0005.1

Cheng, C. T., Chou, C., Lin, P.Y., Hsu, H. H., & Chen, Y. M. (2025) TReAD: 40-year Taiwan Reanalysis Downscaling Dataset at 2 km, SciDM [data set], https://doi.org/10.30193/scidm-rs-2576295

Cheng, F. Y., Hsu, Y. C., Lin, P. L., & Lin, T. H. (2013). Investigation of the effects of different land use and land cover patterns on mesoscale meteorological simulations in the Taiwan area. Journal of applied Meteorology and Climatology, 52(3), 570-587. https://doi.org/10.1175/JAMC-D-12-0109.1

Chen, Y. Y., Huang, W., Wang, W. H., Juang, J. Y., Hong, J. S., Kato, T., & Luyssaert, S. (2019). Reconstructing Taiwan's land cover changes between 1904 and 2015 from historical maps and satellite images. Scientific reports, 9(1), 3643. https://doi.org/10.1038/s41598-019-40063-1

Chen, F., & Dudhia, J. (2001). Coupling an advanced land surface–hydrology model with the Penn State–NCAR MM5 modeling system. Part I: Model implementation and sensitivity. Monthly weather review, 129(4), 569-585. https://doi.org/10.1175/1520-0493(2001)129<0569:CAALSH>2.0.CO;2

Danielson, J. J., & Gesch, D. B. (2011). Global multi-resolution terrain elevation data 2010 (GMTED2010) (No. 2011-1073). US Geological Survey. https://doi.org/10.3133/ofr20111073

Ebita, A., Kobayashi, S., Ota, Y., Moriya, M., Kumabe, R., Onogi, K., ... & Ishimizu, T. (2011). The Japanese 55-year reanalysis "JRA-55": an interim report. Sola, 7, 149-152. https://doi.org/10.2151/sola.2011-038

Hong, S.-Y., and H. L. Pan, 1996: Nonlocal boundary layer vertical diffusion in a medium-range forecast model. *Mon. Wea. Rev.*, 124, 2322 – 2339. https://doi.org/10.1175/1520-0493(1996)124%3C2322:NBLVDI%3E2.0.CO;2

He, B. J., Wang, J., Liu, H., & Ulpiani, G. (2021). Localized synergies between heat waves and urban heat islands: Implications on human thermal comfort and urban heat management. Environmental Research, 193, 110584. https://doi.org/10.1016/j.envres.2020.110584

Hersbach, H., Bell, B., Berrisford, P., Biavati, G., Horányi, A., Muñoz Sabater, J., Nicolas, J., Peubey, C., Radu, R., Rozum, I., Schepers, D., Simmons, A., Soci, C., Dee, D., Thépaut, J-N., 2018a: ERA5 hourly data on pressure levels from 1979 to present. Copernicus Climate Change Service (C3S) Climate Data Store (CDS). (Accessed on 01-12-2019)

Hersbach, H., Bell, B., Berrisford, P., Biavati, G., Horányi, A., Muñoz Sabater, J., Nicolas, J., Peubey, C., Radu, R., Rozum, I., Schepers, D., Simmons, A., Soci, C., Dee, D., Thépaut, J-N., 2018b: ERA5 hourly data on single levels from 1979 to present. Copernicus Climate Change Service (C3S) Climate Data Store (CDS). (Accessed on 01-12-2019)

https://doi.org/10.5194/essd-2026-242
Preprint. Discussion started: 20 April 2026

Hersbach, H, Bell, B, Berrisford, P, et al. The ERA5 global reanalysis. *Q J R Meteorol Soc*. 2020: 146, 1999–2049. https://doi.org/10.1002/qj.3803

Iacono, M. J., Delamere, J. S., Mlawer, E. J., Shephard, M. W., Clough, S. A., & Collins, W. D. (2008). Radiative forcing by long-lived greenhouse gases: Calculations with the AER radiative transfer models. Journal of Geophysical Research: Atmospheres, 113(D13). https://doi.org/10.1029/2008JD009944

Kain, J. S., and J.M. Fritsch, 1990: A one-dimensional entraining/detraining plume model and its application in convective parameterization. *J. Atmos. Sci*., 47,2784-2802. https://doi.org/10.1175/1520-0469(1990)047%3C2784:AODEPM%3E2.0.CO;2

Kain, J. S. (2004). The Kain–Fritsch convective parameterization: an update. Journal of applied meteorology, 43(1), 170-181, doi:10.1175/1520-0450(2004)043<0170:TKCPAU>2.0.CO;2

Kalnay, E., Kanamitsu, M., Kistler, R., Collins, W., Deaven, D., Gandin, L., Iredell, M., Saha, S., White, G., Woollen, J., Zhu, Y., Chelliah, M., Ebisuzaki, W., Higgins, W., Janowiak, J., Mo, K. C., Ropelewski, C., Wang, J., Leetmaa, A., Reynolds, R., Jenne, R., and Joseph, D., 1996: The NCEP/NCAR 40-Year Reanalysis Project, B. Am. Meteorol. Soc., 77, 437–472

Kanamitsu, M., W. Ebisuzaki, J. Woollen, S. K. Yang, J. J. Hnilo, M. Fiorino, and G. L. Potter, 2002: NCEP-DOE AMIP-II Reanalysis (R-2). Bull. Amer. Meteor. Soc., 83, 1631-1643. https://doi.org/10.1175/BAMS-83-11-1631

Kanamitsu, M., & Kanamaru, H. (2007). Fifty-seven-year California Reanalysis Downscaling at 10 km (CaRD10). Part I: System detail and validation with observations. Journal of Climate, 20(22), 5553-5571. https://doi.org/10.1175/2007JCLI1482.1

Kanamaru, H., & Kanamitsu, M. (2007). Fifty-seven-year California reanalysis downscaling at 10 km (CaRD10). Part II: Comparison with North American regional reanalysis. Journal of Climate, 20(22), 5572-5592.

Kayaba, N., Yamada, T., Hayashi, S., Onogi, K., Kobayashi, S., Yoshimoto, K., ... & Yamashita, K. (2016). Dynamical regional downscaling using the JRA-55 reanalysis (DSJRA-55). Sola, 12, 1-5. https://doi.org/10.2151/sola.2016-001

Kobayashi, S., Ota, Y., Harada, Y., Ebita, A., Moriya, M., Onoda, H., ... & Takahashi, K. (2015). The JRA-55 reanalysis: General specifications and basic characteristics. Journal of the Meteorological Society of Japan. Ser. II, 93(1), 5-48. https://doi.org/10.2151/jmsj.2015-001

Lynch, P., & Huang, X. Y. (1992). Initialization of the HIRLAM model using a digital filter. Monthly Weather Review, 120(6), 1019-1034.https://doi.org/10.1175/1520-0493(1992)120%3C1019:IOTHMU%3E2.0.CO;2

Lin, C. Y., Chen, F., Huang, J. C., Chen, W. C., Liou, Y. A., Chen, W. N., & Liu, S. C. (2008). Urban heat island effect and its impact on boundary layer development and land–sea circulation over northern Taiwan. Atmospheric Environment, 42(22), 5635-5649. https://doi.org/10.1016/j.atmosenv.2008.03.015

Lim, K. S. S., & Hong, S. Y. (2010). Development of an effective double-moment cloud microphysics scheme with prognostic cloud condensation nuclei (CCN) for weather and climate models. Monthly weather review, 138(5), 1587-1612. https://doi.org/10.1175/2009MWR2968.1

https://doi.org/10.5194/essd-2026-242
Preprint. Discussion started: 20 April 2026

686 Liu, W. B., Peh, H. C., Wang, C. K., Mangwe, M. C., Chen, C. F., & Chiang, H. I. (2018). Effect of seasonal
687 changes on fertility parameters of Holstein dairy cows in subtropical climate of Taiwan. Asian-
688 Australasian journal of animal sciences, 31(6), 820. doi: 10.5713/ajas.17.0301

689 Lo, J. C.-F., Yang, Z.-L., and Pielke, R. A., 2008: Assessment of three dynamical climate downscaling methods
690 using the weather research and forecasting (WRF) model. *J. Geophys. Res.,* 113 (D9), D09112.
691 doi:10.1029/2007jd009216

692 Luo, W., Taylor, M. C., & Parker, S. R. (2008). A comparison of spatial interpolation methods to estimate
693 continuous wind speed surfaces using irregularly distributed data from England and Wales. International
694 Journal of Climatology: A Journal of the Royal Meteorological Society, 28(7), 947-959.
695 https://doi.org/10.1002/joc.1583

696 Memon, R. A., Leung, D. Y., & Liu, C. H. (2010). Effects of building aspect ratio and wind speed on air
697 temperatures in urban-like street canyons. Building and Environment, 45(1), 176-188.
698 https://doi.org/10.1016/j.buildenv.2009.05.015

699 Monin, A. S., & Obukhov, A. M. (1954). Osnovnye zakonomernosti turbulentnogo peremeshivanija v
700 prizemnom sloe atmosfery (Basic laws of turbulent mixing in the atmosphere near the ground). Trudy
701 geofiz. inst. AN SSSR, 24(151), 163-187.

702 Mlawer, E.J., S.J. Taubman, P.D. Brown, M.J. Iacono, and S.A. Clough, 1997: Radiative transfer for
703 inhomogeneous atmospheres: RRTM, a validated correlated-k model for the longwave, *J. Geophys. Res.*,
704 102,16,663–82 , doi:10.1029/97JD00237.

705 Saha, S., Moorthi, S., Pan, H., Wu, X., Wang, J., Nadiga, S., Tripp, P., Kistler, R., Woollen, J., Behringer, D.,
706 Liu, H., Stokes, D., Grumbine, R., Gayno, G., Wang, J., Hou, Y., Chuang, H., Juang, H. H., Sela, J.,
707 Iredell, M., Treadon, R., Kleist, D., Van Delst, P., Keyser, D., Derber, J., Ek, M., Meng, J., Wei, H., Yang,
708 R., Lord, S., van den Dool, H., Kumar, A., Wang, W., Long, C., Chelliah, M., Xue, Y., Huang, B.,
709 Schemm, J., Ebisuzaki, W., Lin, R., Xie, P., Chen, M., Zhou, S., Higgins, W., Zou, C., Liu, Q., Chen, Y.,
710 Han, Y., Cucurull, L., Reynolds, R. W., Rutledge, G., & Goldberg, M. (2010). The NCEP Climate
711 Forecast System Reanalysis. Bulletin of the American Meteorological Society, 91(8), 1015-1058.
712 https://doi.org/10.1175/2010BAMS3001.1

713 Skamarock, W. C., & Klemp, J. B. (2008). A time-split nonhydrostatic atmospheric model for weather research
714 and forecasting applications. Journal of computational physics, 227(7), 3465-3485.
715 https://doi.org/10.1016/j.jcp.2007.01.037

716 Ulpiani, G. (2021). On the linkage between urban heat island and urban pollution island: Three-decade
717 literature review towards a conceptual framework. Science of the total environment, 751, 141727.
718 https://doi.org/10.1016/j.scitotenv.2020.141727

719 Wang, S. Y., Ou, H. Y., Chen, P. C., & Lin, T. P. (2024). Implementing policies to mitigate urban heat islands:
720 Analyzing urban development factors with an innovative machine learning approach. Urban Climate, 55,
721 101868. https://doi.org/10.1016/j.uclim.2024.101868

722 Weng, S. P., & Yang, C. D. (2018). The construction and verification of daily gridded rainfall dataset (1960–
723 2015) in Taiwan. Taiwan Water Conserv, 66, 33-52.

724 Yang, X. (2005). Analysis blending using a spatial filter in grid-point model coupling. Hirlam Newsletter, 48,
725 49-55.

726